



Cite this: *Green Chem.*, 2025, **27**, 14658

## Nordic microalgae immobilized to a sulfur-cooking oil copolymer form a highly efficient, sustainable and reusable sorbent to remove heavy metals from complex mixtures

Antonio Leon-Vaz,  <sup>†a,b</sup> Martin Plöhn,  <sup>†a</sup> Juan Cubero-Cardoso,  <sup>c,d,e</sup> Juan Urbano  <sup>c</sup> and Christiane Funk  <sup>\*a</sup>

Heavy metal contamination is of highest concern for the environment. Bioremediation, using microorganisms to adsorb and enrich heavy metals, offers an outstanding solution, especially when the pollutants appear at concentrations where physical/chemical methods are not efficient. This study presents a sustainable approach to heavy metal removal through the development of a microalgae-based sorbent supported on a copolymer produced entirely from recycled waste streams. The copolymer was synthesized by inverse vulcanization using sulfur recovered from petrochemical waste and waste cooking oil, demonstrating a circular use of industrial and household by-products. This sustainable, biobased sorbent was highly efficient in removing the heavy metals copper, cadmium and lead in a multi-element mixture at concentrations of industrial relevance. Kinetics and equilibrium parameters and even adsorption capacities improved drastically after immobilization of microalgae to the copolymer, compared to free-swimming microalgae or copolymer alone. The green microalga *Chlorella vulgaris* (13-1) immobilized to the copolymer removed more than 95% of the total Cu<sup>2+</sup> and Cd<sup>2+</sup> and 50% of the total Pb<sup>2+</sup> within 8 h. Additionally, this sorbent is reusable; a desorption and regeneration step with 0.1M EDTA and CaCl<sub>2</sub> allowed up to 98% recovery of the concentrated, bound heavy metals. Reusing the microalgal-copolymer sorbent in a second removal cycle resulted in removal rates of 75–99% of the initial ones. This novel sorbent allows not only sustainable and efficient removal of heavy metal mixtures from industrial wastewaters but also can be used in subsequent rounds during wastewater purification.

Received 22nd July 2025,  
Accepted 23rd October 2025

DOI: 10.1039/d5gc03769g

rsc.li/greenchem

### Green foundation

1. This study presents a novel sorbent composed of Nordic microalgae immobilized on an inverse-vulcanization copolymer synthesized from sulfur and cooking oil – both low-cost and waste-derived materials – designed for efficient removal of heavy metals from mixtures.
2. Within eight hours, the microalgal-copolymer sorbent removed more than 95% of Cu<sup>2+</sup> and Cd<sup>2+</sup> and approximately 50% of Pb<sup>2+</sup> from aqueous solutions. In a subsequent removal cycle, 75–99% of the initial efficiency was achieved, validating the reusability of the sorbent and its practical applicability in repeated bioremediation processes.
3. Further research should address process scale-up and optimization of heavy metal recovery, including system reusability, metal purification, and downstream valorization.

<sup>a</sup>Department of Chemistry, Umeå University, 901 87 Umeå, Sweden.

E-mail: christiane.funk@umu.se

<sup>b</sup>Laboratory of Biochemistry, Faculty of Experimental Sciences and REMSMA, University of Huelva, 210071 Huelva, Spain

<sup>c</sup>Laboratory of Sustainable and Circular Technology, CIDERTA and Chemistry Department, Faculty of Experimental Sciences University of Huelva, 21071 Huelva, Spain

<sup>d</sup>Institute of Water Research, University of Granada, Granada 18071, Spain

<sup>e</sup>Department of Microbiology, Pharmacy Faculty, University of Granada, Campus de Cartuja s/n, Granada 18011, Spain

<sup>†</sup>These authors contributed equally to the work.

## 1. Introduction

Heavy metals are extremely hazardous environmental pollutants due to their high toxicity, ubiquity, and persistence. Because of their capacity to bio-accumulate and biomagnify, these elements cause serious problems in aquatic ecosystems and thereby also to human health.<sup>1,2</sup> Heavy metal contamination is mainly produced by anthropogenic activities; industrial or mining effluents cause acidification and accumulation of these compounds not only in rivers, lakes and the sea, but



also in aquifers all over the world.<sup>3,4</sup> In addition to anthropogenic sources, geochemical cycles play a significant role in contributing to this contamination. The Tinto River in Huelva (southwestern Spain) serves as a striking example, where an underground bioreactor naturally generates substantial levels of sulfides and heavy metals, maintaining an acidic environment with pH values between 2 and 3.<sup>5</sup> Chromium, cadmium, arsenic, lead and zinc are the most common heavy metals produced by industrial or mining activities in Scandinavia. These elements often appear as a mix at low concentrations (0.1–5 mg L<sup>-1</sup>) in industrial waste streams, which complicates their removal using conventional techniques, such as chemical precipitation, flocculation or membrane filtration.<sup>6</sup>

Bioremediation with the help of microorganisms emerges as a promising solution to eliminate heavy metal contamination from aquatic ecosystems. Microalgae are a group of microscopic organisms able to grow in freshwater or marine ecosystems and due to their photosynthetic activity they produce about 50% of the atmospheric oxygen and convert the greenhouse gas CO<sub>2</sub> into biomass.<sup>7,8</sup> Due to their metabolic adaptability, several species can be cultivated in municipal or industrial wastewaters containing heavy metal contamination.<sup>9,10</sup> Various microalgal strains have been tested for their potential to be used in heavy metal bioremediation processes. While most strains can remove heavy metals when exposed to a single element, their adsorption capacities decrease when grown in a mixture of two elements.<sup>11</sup> However, studies on more complex mixtures of heavy metals are scarce. Native Nordic microalgae, adapted to the harsh Scandinavian climate, are highly resistant to various stress conditions<sup>12</sup> and therefore are promising organisms for heavy metal bioremediation.<sup>13</sup>

Immobilization of microalgae, *i.e.* trapping or attaching them to a support matrix, enhances their remediation efficiency by increasing population density and facilitating easy separation from the medium. This promising technique was shown not only to improve the capacity of microalgae to remove pollutants but also to increase their economic value due to lower costs of biomass harvesting and recovery.<sup>11,14</sup> Common immobilization matrices used in microalgal-based wastewater treatment are alginate, sponge or activated carbon.<sup>15–17</sup> The cyanobacterium *Synechocystis* sp. PCC6803 was immobilized in spores of the fungus *Aspergillus fumigatus* and was able to remove 90% of the total cadmium and 80% of the total chromium from the medium containing initial concentrations of 1 mg L<sup>-1</sup>.<sup>18</sup>

Biosorption is possible due to the unique and complex structure of the microalgal cell wall. The variety of functional groups on the surface of the cell wall can act as binding sites for heavy metals, thus removing them from the environment.<sup>19</sup> However, because the microalgal cell wall structure greatly varies between strains and is influenced by growth conditions,<sup>20</sup> it is vital to develop a scaffold able to attach different types of microalgal species.<sup>19</sup> Furthermore, for industrial applications, it is important to investigate sustainable scaffolds that, after microalgal immobilization, can be reused

multiple times and effectively remove several heavy metals under conditions that closely resemble real-world scenarios. Copolymers synthesized by inverse vulcanization offer such a versatile and sustainable solution as scaffolds. These compounds are produced by a reaction to achieve hybrid inorganic–organic polymeric materials, in which the S<sub>8</sub> ring opens and polymerization can occur with other unsaturated cross-linkers.<sup>21</sup> Combining recycled sulfur (S<sub>8</sub>) from the petrochemical industry with unsaturated molecules, such as used cooking oil waste (CKO)<sup>22</sup> yields a copolymer with remarkable properties, while also making it both sustainable and compostable. In cooking oil, about 85% of the fatty acids contain double bonds, facilitating a reaction with sulfur atoms generating a hybrid copolymer (S/CKO) by inverse vulcanization.<sup>23</sup> Furthermore, cooking oil waste has become a significant environmental problem; its improper disposal causes pollution of water sources and the release of harmful greenhouse gases. Thus, the combination of industrial- and kitchen-waste could offer an outstanding and sustainable scaffold to immobilize Nordic microalgae for bioremediation of heavy metals.

In this work, six different Nordic microalgal strains were exposed to complex heavy metal mixtures containing copper, cadmium and lead, and their tolerances and removal capacities were studied. The Nordic culture collection at Umeå University contains strains, which have been selected based on their ability to grow in municipal wastewater. Six of these free-swimming strains, *Coelastrella* sp. (3-4), *Chlorella sorokiniana* (2-21-1), *Chlorella vulgaris* (13-1), *Micractinium* sp. (P9-1), *Scenedesmus obliquus* (13-8) and *Scotiellopsis reticulata* (UFA-2) had previously demonstrated high tolerance and biosorption capacity towards Cd<sup>2+</sup> as single element,<sup>13</sup> but still differed in morphology and cell surface.<sup>20</sup> While three strains (3-4, 13-1, and 2-21-1) displayed spherical morphologies, the other strains exhibited oval to cylindrical forms (P9-1, 13-8 and UFA-2).<sup>24</sup> Such differences in morphology and cell surfaces provide opportunities to develop tailored strategies for the immobilization within the S/CKO copolymer matrix. Furthermore, these strains were immobilized onto a sulfur/cooking oil copolymer and the novel microalgal-copolymer sorbent was used to remove mixtures of these heavy metals in various concentrations. Removal kinetics and equilibrium parameters were determined. Finally, the recovery of heavy metals from the microalgal-copolymer sorbent and its reusability in a second round of heavy metal removal was determined. Our data demonstrate that Nordic microalgae immobilized to an S/CKO copolymer form a promising sorbent, effectively removing heavy metal mixtures at industrially relevant concentrations, which is reusable in subsequent removal cycles.

## 2. Experimental

### 2.1. Synthesis of copolymer

Hybrid copolymers have been synthesized by elemental sulfur (S) from the Cepsa SA petrochemical company, and cooking oil



(CKO) from kitchen wastes. Synthesis of the S/CKO: 80/20 (w/w) copolymer was carried out as described in León-Vaz *et al.*<sup>25</sup> for sulfur/castor oil copolymers.

## 2.2. Copolymer characterization

The oil samples underwent transesterification with KOH in methanol to determine their fatty acid composition. The resulting fatty acid methyl esters were analysed using a Hewlett-Packard 6890 Series gas chromatograph (GC) that was fitted with a DB-23 fused silica capillary column (60 m × 0.25 mm, i.d. 0.25 μm film thickness) and a flame ionization detector (FID). The detector and injector temperatures were kept at 240 °C, while the column temperature was held at an isothermal oven temperature of 185 °C. The fatty acid methyl ester percentages were calculated based on the peak areas and retention times. The mass fractions of each fatty acid were expressed as a percentage.

The copolymer was further analysed by Diffuse Reflectance Infrared Fourier Transform Spectroscopy (FTIR). After mixing the copolymer with KBr the spectra were recorded in a range of 400–4000 cm<sup>-1</sup> with a spectral resolution of 4 cm<sup>-1</sup> using the OPUS Software (Ver. 6.5) of the equipment.

Raman spectra were recorded on a Renishaw Qontor system (Renishaw Plc, New Mills, Wotton-under-Edge, Gloucestershire, GL12 8JR, UK), using a 405 nm laser and 2400 lines per mm grating. Laser intensity was set to a nominal 4 mW (10% of maximum power at laser output) and exposure time at 0.1 s. The laser was focused on the sample *via* a 5× lens, and spectra were recorded in static mode, with the centre set at 1400 cm<sup>-1</sup>. 136 spectra were recorded over an 8 × 17 rectangular grid pattern with 50 μm steps in between each position (in XY direction), while the Z level was kept constant. Spectra were subjected to cosmic ray removal and 4-component noise filtering using the built-in scripts of Renishaw's WiRE software (version 5.3, build 13318, Renishaw Plc, New Mills, Wotton-under-Edge, Gloucestershire, GL12 8JR, UK). Spectra were exported as ASCII text files.

Solid-state <sup>13</sup>C Nuclear Magnetic Resonance (NMR) Spectroscopy was acquired with a Bruker Avance III HD 400 MHz (Rheinstetten, Germany) at a frequency of 100.63 MHz using zirconium rotors with a 4 mm outside diameter.

## 2.3. Microalgal cultivation

The Nordic microalgae described in this work, *Coelastrella* sp. (3-4), *Chlorella sorokiniana* (2-21-1), *Chlorella vulgaris* (13-1), *Micractinium* sp. (P9-1), *Scenedesmus obliquus* (13-8) and *Scotiellopsis reticulata* (UFA-2),<sup>26</sup> were cultured in Tris-Acetate-Phosphate (TAP) medium.<sup>27</sup> Microalgal pre-inocula were added to the medium at the initial optical density OD<sub>660</sub> of 0.2 for tolerance experiments. In the single heavy metal experiment, CuSO<sub>4</sub>, CdSO<sub>4</sub> or PbSO<sub>4</sub> were added to the culture medium at concentrations between 5 and 10 mg L<sup>-1</sup> of Cu<sup>2+</sup>, 1 and 5 mg L<sup>-1</sup> of Cd<sup>2+</sup>, and 0.6 and 3.6 mg L<sup>-1</sup> of Pb<sup>2+</sup>. These concentrations were selected based on Scandinavian heavy metal

pollutions detected in lakes.<sup>4</sup> Heavy metal concentrations in mixtures are shown in Table S1. The metals were added after autoclaving, and pH was adjusted to 6.0. The microalgae were cultured at 20 °C under continuous agitation (100 rpm) and light irradiation (100 μmol m<sup>-2</sup> s<sup>-1</sup>).

## 2.4. Microalga-copolymer sorbent

To obtain the sorbent, a microalgal pre-inoculum was cultivated for 3 days. The microalgae (at a concentration of 1 g L<sup>-1</sup>) were then resuspended in 50 mL of TAP medium. S/CKO copolymer was added at a concentration of 20 g L<sup>-1</sup> and mixed by agitation before adding the heavy metal mix. Immobilization of the microalgae to the copolymer was confirmed by Scanning Electron Microscope-imaging. Samples of the corresponding cultures from different time points (0, 2, and 24 h) were prepared as reported in Malyshev *et al.*<sup>28</sup>

## 2.5. Adsorption studies

Adsorption of copper, cadmium and/or lead to either the S/CKO copolymer, Nordic microalgae or the microalgae-copolymer sorbent were tested in biological triplicates. The microalgae, copolymer or microalga-copolymer sorbent were kept at pH 6.0 and 20 °C under continuous agitation (100 rpm) and light irradiation (100 μmol m<sup>-2</sup> s<sup>-1</sup>) for 24 h.

## 2.6. Kinetic and equilibrium parameters of metal adsorption

At specific time points (after 0, 1, 3, 5, 7, 10, 15, 30, 60, 120, 240, 480 and 1440 min) 2 mL samples were removed and centrifuged immediately at 20 000g for 2 min at 4 °C to separate the supernatant from the biomass. Afterwards liquid samples were acidified in 1% HNO<sub>3</sub>, filtered through 0.2 μm syringe filters and stored at 4 °C until further analysis.

To model the adsorption isotherms at equilibrium the microalgal strains, the copolymer and the microalgae-copolymer sorbent were exposed to increasing concentrations of heavy metals for 6 h at 20 °C. Each adsorbent was tested individually in the presence of either 0.25, 0.5, 1, 2.5, 5, 10 and 25 mg L<sup>-1</sup> of the heavy metals. After that time, 2 mL samples were centrifuged, acidified and filtered as described above. All concentrations were tested as triplicates against a control, which contained the same heavy metal concentrations but no adsorbent.

## 2.7. Modelling heavy metals kinetic and equilibrium

Several models were applied to describe first the adsorption kinetics under non-equilibrium conditions and then the isotherm models under equilibrium conditions. Pseudo-first and pseudo-second order kinetic models were used to describe the non-equilibrium process. For the isotherm models the Langmuir-, Freundlich-, Sips- and Dubinin-Radushkevich-equations have been applied on the recorded data. All calculations have been performed as previously described in Plöhn *et al.*<sup>13</sup> Curves were fitted in GraphPad Prism (Version 10.0.0) *via* Non-Linear Least Square regression (NLLS).



## 2.8. Desorption of heavy metals

To recover the heavy metals from the microalgae-copolymer sorbent a modified protocol based on Li *et al.* and Ding *et al.*<sup>29,30</sup> was applied. After heavy metal adsorption the sorbent was separated from the liquid and washed with distilled water. Afterwards the sorbent was transferred to a desorption solution containing either 0.1 M HNO<sub>3</sub> or 0.1 M EDTA. After 1 h, the sorbent was again separated from liquid and washed before transferring it into a 0.1 M CaCl<sub>2</sub>-regeneration solution for another hour. After washing with distilled water, the regenerated sorbent was suspended in the corresponding heavy metal solution (second round) to analyse its reusability.

## 2.9. Heavy metal determination

Trace element signals were determined measuring optical emission spectra after ionization by an Inductively Coupled Plasma (ICP-OES, Agilent Technologies 7800). All samples were filtered and diluted with 1% HNO<sub>3</sub> trace metal grade. Trace metal concentrations were then calculated with the help of a 10-calibration point curve covering concentrations between 0–25 mg L<sup>-1</sup> of the corresponding element. The calibration curves were measured prior to the samples to allow correct wavelength assignment.

## 2.10. Statistical analysis

All measurements were carried out in triplicates and represented as mean value ± SD. Significant differences were considered for values with *p* < 0.05. Statistical analyses were performed using GraphPad Prism (Version 10.0.0).

# 3. Results

## 3.1. Characterization of the sustainable S/CKO copolymer

The S/CKO copolymer used as a scaffold to immobilize Nordic microalgae was made from recycled cooking oil containing total proportions of fatty acids as follows: oleic (64%), linoleic (17%), palmitic (11%), stearic (3.9%), ascleptic (2.6%), palmitoleic (0.7%), arachidic (0.4%), linolenic (0.4%) and docosanoic (0.2%) being these percentages comparable with olive oil.<sup>31</sup>

The characterization of the copolymer structure was performed using FTIR, Raman, and solid <sup>13</sup>C-NMR spectroscopy (Fig. 1). The FTIR spectrum of the copolymer (Fig. 1A) displays prominent peaks corresponding to groups such as (–OH) at 3500 cm<sup>-1</sup>, (–CH<sub>2</sub>) at 2900 cm<sup>-1</sup>, and (–C=O) at 1745 cm<sup>-1</sup>. The lack of detectable peaks typically associated with double bonds (*i.e.*, at 1400 and 3000 cm<sup>-1</sup>), which are expected in the vegetable cooking oil, suggests complete reactions with sulfur. The successful co-monomer conversion<sup>32</sup> was confirmed by the peak associated with S–S stretching at 465 cm<sup>-1</sup> (Fig. 1A), which is consistent to spectra of polysulfide materials. Raman spectrum provided a better indication of the high sulfur percentage present in the copolymer (Fig. 1B). The strong signals at 219 and 474 cm<sup>-1</sup> correspond to S–S bonds, while very weak

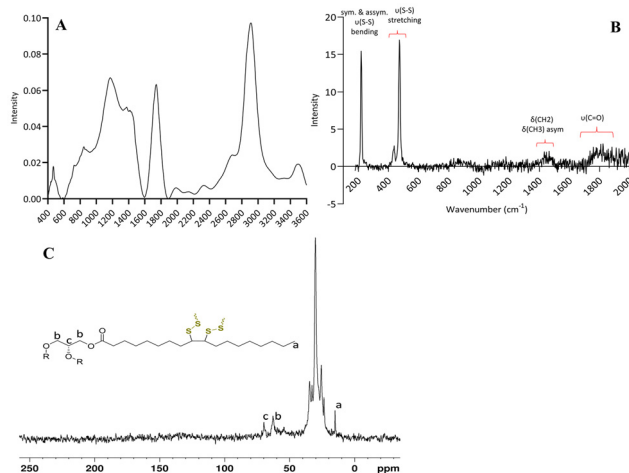


Fig. 1 FTIR spectrum (A), Raman spectrum (B), and Solid-state <sup>13</sup>C-NMR spectrum (C) of the hybrid (S/CKO) copolymer.

signals at 1440 and 1750 cm<sup>-1</sup> indicate the vegetable oil domain. The solid-state <sup>13</sup>C-NMR spectrum of the copolymer revealed the presence of distinctive vegetable oil peaks, with the first peak observed at  $\delta = 14$ , corresponding to the terminal carbon of the fatty acyl chain (Fig. 1C). Additional characteristic peaks were identified in the  $\delta = 20$ –40 range, representing various carbon atoms of the fatty acid chains, and two peaks associated with glycerol were observed at  $\delta = 61$  and  $\delta = 68$ . Notably, no further signals were detected beyond these peaks, including those associated with double bonds of unsaturated fatty acids, which have been reported in previous studies.<sup>33</sup>

## 3.2. Tolerance of free-swimming Nordic microalgae to heavy metals and their removal capacities

To investigate the tolerance to heavy metals and to determine their sublethal concentrations, the growth rates of Nordic microalgal strains were measured in the presence of divalent heavy metals at concentrations relevant in industrial wastewaters (copper, 5 mg L<sup>-1</sup> and 10 mg L<sup>-1</sup>; cadmium, 1 mg L<sup>-1</sup> and 5 mg L<sup>-1</sup>; lead, 0.6 L<sup>-1</sup> and 3.6 mg L<sup>-1</sup>)<sup>4</sup> both as single elements and in mixtures. After pre-screenings, six Nordic microalgal strains belonging to different classes were selected: three *Chlorophyceae* species, such as *Coelastrrella* sp. (3-4), *Scenedesmus obliquus* (13-8) and *Scotiellopsis reticulata* (UFA-2); and three *Trebouxiophyceae* species, including *Chlorella sorokiniana* (2-21-1), *Chlorella vulgaris* (13-1) and *Micractinium* sp. (P9-1). Exposure to copper (5 mg L<sup>-1</sup>) led to a slight, but significant decrease in growth rate of the strains UFA-2 (20%), 3-4 (15%), 13-1 (26%) and 2-21-1 (17%) compared to the control cultures grown in standard TAP medium (Fig. 2A). Raising the Cu<sup>2+</sup> concentration to 10 mg L<sup>-1</sup> did not further affect most strains, however, this concentration was highly toxic for P9-1, whose growth rate was reduced by 80% compared to the control (Fig. 2A). Low concentrations of Cd<sup>2+</sup> (1 mg L<sup>-1</sup>) only significantly affected one strain, UFA-2, whose growth rate was diminished by 30% compared to the control cultures. In the



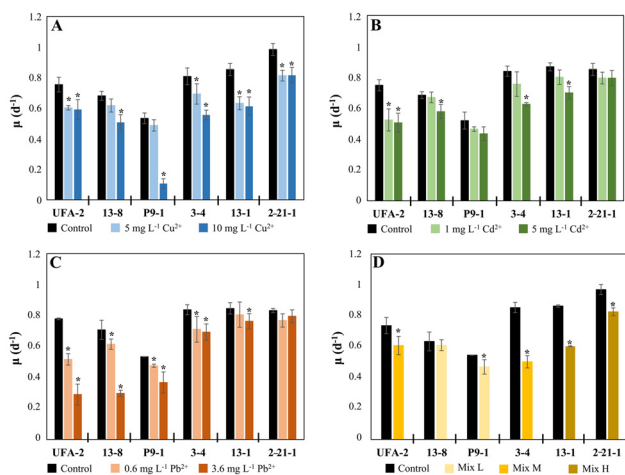


**Fig. 2** Growth rate values (d<sup>-1</sup>) of six free-swimming Nordic microalgae exposed to Cu<sup>2+</sup> (A), Cd<sup>2+</sup> (B), Pb<sup>2+</sup> (C) and a mix of these elements (D). Mix H, high concentrations of heavy metals; Mix M, medium concentrations; Mix L, low concentrations as given in Table S1. Asterisk (\*) indicates a significant difference  $p < 0.05$  between cultures exposed to heavy metal(s) and the control.

presence of high cadmium concentrations (5 mg L<sup>-1</sup>) only 2-21-1 and P9-1 obtained growth rate values similar to the control cultures (Fig. 2B). Exposure to lead significantly affected the growth rates of the strains UFA-2, 13-8, P9-1 and 3-4, independent of the concentration. While low concentrations of Pb<sup>2+</sup> (0.6 mg L<sup>-1</sup>) decreased their growth rates by 33, 15, 10 and 15%, respectively, high concentrations (3.6 mg L<sup>-1</sup>) diminished the growth rates by 63, 60, 30 and 20%, respectively (Fig. 2C). Interestingly, lead did not affect the growth rates of 13-1 and 2-21-1, confirming that *Chlorella* strains possess high tolerance to this heavy metal.

After exposure to single elements, the six Nordic strains were exposed to a mixture of heavy metals at concentrations of 5 mg L<sup>-1</sup> Cu<sup>2+</sup>, 2.5 mg L<sup>-1</sup> Cd<sup>2+</sup> and 3.6 mg L<sup>-1</sup> Pb<sup>2+</sup> (high concentration, Mix H). Under these conditions, only *Chlorella vulgaris* (13-1) and *Chlorella sorokiniana* (2-21-1) were able to grow. Thus, lower heavy metal concentrations were used for the other microalgae. At concentrations of 5 mg L<sup>-1</sup> Cu<sup>2+</sup>, 2 mg L<sup>-1</sup> Cd<sup>2+</sup> and 1.8 mg L<sup>-1</sup> Pb<sup>2+</sup> (medium concentration, Mix M), still 13-8 and P9-1 were not able to grow. Consequently, those two strains were exposed to even lower concentrations of heavy metals (low concentration, Mix L), containing Cu<sup>2+</sup> at 5 mg L<sup>-1</sup>, Cd<sup>2+</sup> at 1 mg L<sup>-1</sup> and Pb<sup>2+</sup> at 1 mg L<sup>-1</sup>. Based on their tolerance to heavy metals, in the upcoming studies 13-1 and 2-21-1 were exposed to Mix H, 3-4 and UFA-2 to Mix M and 13-8 as well as P9-1 to Mix L (Table S1). At these conditions, five out of the six strains displayed significantly decreased growth rates and cell viabilities (Fig. 2D), compared to the control, the growth rate values of the microalgae exposed to heavy metal mixes were reduced by 40% (3-4, Mix M), 30% (13-1, Mix H), 18% (UFA-2, Mix M), 15% (2-21-1, Mix H), 14% (P9-1, Mix L). Only the growth rate of 13-8 was not significantly altered in the presence of heavy metals (4%, Mix L, Fig. 2D).

To determine the adsorption and removal capacities of heavy metals by the microalgae, the six Nordic strains were exposed to single heavy metals (Fig. 3A–C) or to the heavy metal mixtures (Fig. 3D). Nordic microalgae were able to remove moderate concentrations of copper (35–50%) and lead (60–80%) from the aqueous solution (Fig. 3A and C), however, their ability to adsorb cadmium was low. Only around 10% of the initial cadmium concentration was removed by the individual microalgal strains within 24 h (Fig. 3B). The S/CKO copolymer (CP in Fig. 3) was also exposed to the three single heavy metals at different concentrations (Fig. 3A–C). While it was able to remove high amounts of cadmium (40–60%) and lead (around 65%), the copolymer only removed 10–15% of copper. Exposure of either microalgae or copolymer to heavy metal mixtures containing all three elements (Fig. 3D) diminished their removal capacities. Exposed to heavy metal mixtures neither the six Nordic microalgal strains nor the copolymer were able to remove more than 30–40% of the individual heavy metals from the aqueous solution, demonstrating their limitations in industrial relevant multi-elemental mixtures.

### 3.3 Immobilization of microalgae enhances their adsorption capacities to remove heavy metals from multi-elemental mixtures

To enhance the removal performances, immobilization/attachment of Nordic microalga species to the S/CKO copolymer was performed by adding microalgal biomass and copolymer to the culture medium. Scanning electron microscopy (SEM) images of the copolymer before (Fig. 4A) as well as 2 and 24 h after addition of the microalgae (shown *Chlorella vulgaris* (13-1), Fig. 4B and C, respectively) demonstrated successful microalgal immobilisation. The SEM images revealed higher immobilization capacity of the copolymer for 13-1, 3-4 and 2-21-1 after 24 h (Fig. 4C, F and G, respectively) than for UFA-2 and 13-8 (Fig. 4D and E, respectively), demonstrating the high ver-

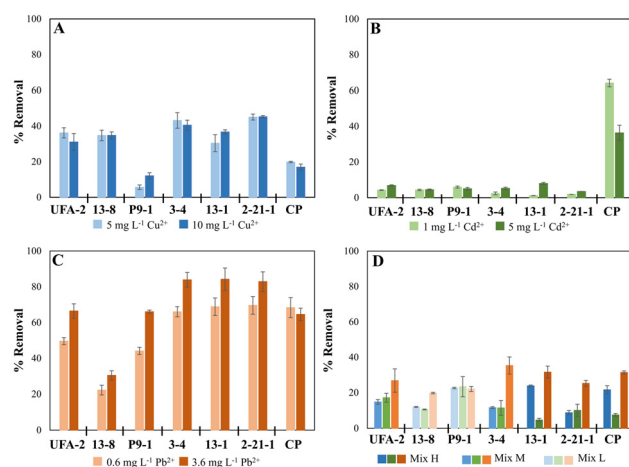


**Fig. 3** Percentage of heavy metal removal by the six free-swimming microalgal strains or the copolymer (CP) exposed to different concentrations of either Cu<sup>2+</sup> (A), Cd<sup>2+</sup> (B), Pb<sup>2+</sup> (C) or mixtures (Table S1) of the three heavy metals (D) for 24 h.



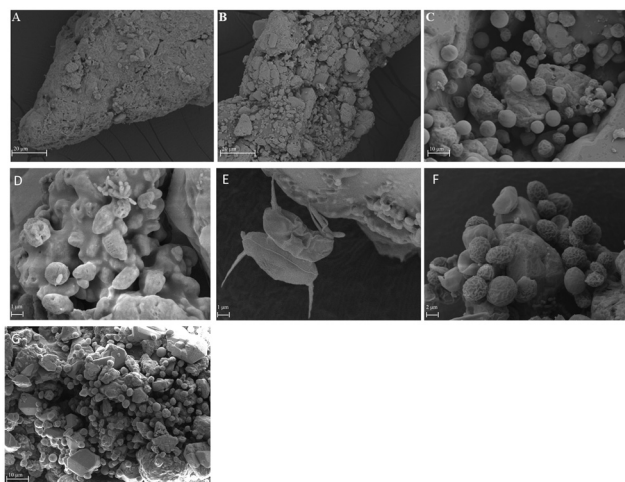


**Fig. 4** Scanning electron microscopy (SEM) images of the S/CKO copolymer before immobilisation (A), as well as 2 h (B) and 24 h (C) after addition of *Chlorella vulgaris* (13-1); 24 h after addition of *Scotiellopsis reticulata* (UFA-2, D), *Scenedesmus obliquus* (13-8, E), *Coelastrella* sp. (3-4, F) and *Chlorella sorokiniana* (2-21-1, G). Magnifications: 2590x for A and B, 3000x for C and G, 15 000x for D and E, and 7950x for F.

sativity of the copolymer, which was able to immobilise all the strains.

Microalgal strains and copolymer were then incubated in the presence of heavy metal mixtures containing  $\text{Cd}^{2+}$ ,  $\text{Cu}^{2+}$  and  $\text{Pb}^{2+}$  at concentrations as tested previously (Mix H, Mix M, Mix L, Table S1). The heavy metal concentrations in solution were analysed before addition of heavy metals (time point 0) and after 1 min, 3 min, 5 min, 7 min, 10 min, 15 min, 30 min, 1 h, 2 h, 4 h, 8 h and 24 h. Fig. 5 presents a comparison of heavy metal removal by *Chlorella vulgaris* (13-1) from a multi-element mixture, illustrating the effects of immobilization onto the copolymer (Fig. 5D–F) versus free-swimming cells (Fig. 5A–C). Removal rates of the other microalgal strains are shown in Fig. S1–S5.

Removal of the three heavy metals in a multi-elemental mixture by free-swimming *Chlorella vulgaris* (13-1) was limited. Within the first hours, a moderate decrease of the heavy metal concentrations was observed (Fig. 5A–C). While  $\text{Cd}^{2+}$  adsorption lasted over a time course of 8 hours (Students *t*-test:  $p_{\text{Cd}} = 0.0249$ ) (Fig. 5A),  $\text{Cu}^{2+}$  ions were adsorbed much faster, and after 2 h the adsorption process was regressing significantly (2–8 h:  $p_{\text{Cu}} = 0.0865$ ) (Fig. 5B). In this slow 2<sup>nd</sup> phase most likely not only adsorption but probably also absorption (2–24 h:  $p_{\text{Cu}} = 0.0222$ ) took place.  $\text{Pb}^{2+}$  ions (Fig. 5C) were rapidly adsorbed within the first hour before regression. Over the time course of 24 hours, around 5% of the  $\text{Cd}^{2+}$  ions, around 24% of  $\text{Cu}^{2+}$  and around 32% of  $\text{Pb}^{2+}$  were removed by *Chlorella vulgaris* (13-1) (Students *t*-tests:  $p_{\text{Cd}} = 0.0292$ ,  $p_{\text{Cu}} = 0.0009$  and  $p_{\text{Pb}} = 0.0036$ ). *Chlorella vulgaris* (13-1) immobilized to the copolymer performed far better; removal of  $\text{Cd}^{2+}$  and  $\text{Cu}^{2+}$  no longer displayed the typical two-phase process ( $R^2_{\text{Cd}} = 0.929$  and  $R^2_{\text{Cu}} = 0.949$ ) (Fig. 5D and E) but instead followed a sigmoidal curve fitting over time ( $R^2_{\text{Cd}} = 0.990$  and  $R^2_{\text{Cu}} =$

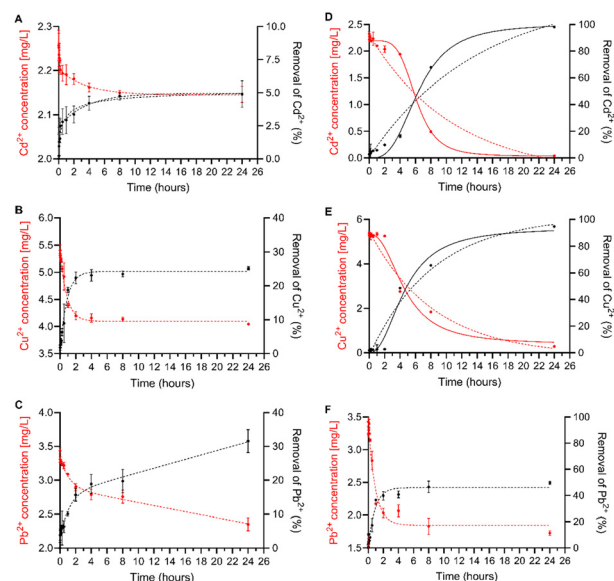


**Fig. 5** Removal of  $\text{Cd}^{2+}$  ( $5 \text{ mg L}^{-1}$ ),  $\text{Cu}^{2+}$  ( $2.5 \text{ mg L}^{-1}$ ), and  $\text{Pb}^{2+}$  ( $3.6 \text{ mg L}^{-1}$ ) from a multi-element mixture by *Chlorella vulgaris* (13-1), comparing free-swimming cells (A–C) and the microalga-copolymer sorbent (D–F). Mean  $\pm$  SD of three biological replicates. Dashed lines represent the fitted curves of two-phase association (black) and decay (red). Solid lines in D and E show the sigmoidal curve fitting for removal of the corresponding elements.

0.977). Additionally, much higher removal rates were observed. The *Chlorella vulgaris* (13-1)-copolymer sorbent was able to remove around 98% of the  $\text{Cd}^{2+}$  and almost 95% of the  $\text{Cu}^{2+}$  from the aqueous phase (Students *t*-tests:  $p_{\text{Cd}} = 0.0001$  and  $p_{\text{Cu}} = 0.0002$ ). The removal of  $\text{Pb}^{2+}$  followed a two-phase decay, as in the absence of copolymer, and was improved by a factor of 1.6 in the microalgal-copolymer sorbent. Additionally, almost 50% of  $\text{Pb}^{2+}$  were removed by immobilized *Chlorella vulgaris* (13-1) (Fig. 5F). Removal rates by the other microalgal strains also enhanced after immobilization (Fig. S1–S5). Removal rates of  $\text{Cd}^{2+}$  and  $\text{Cu}^{2+}$  ( $p_{\text{Cd}} = 0.002$  and  $p_{\text{Cu}} = 1.46 \times 10^{-5}$ ) by *C. sorokiniana* (2-21-1) were significantly improved by a factor of 6.8 and 4, respectively (Fig. S5), while removal of  $\text{Pb}^{2+}$  improved by a factor of 1.3. Removal rates by *Coelastrella* sp. (3-4) immobilized to the copolymer increased for  $\text{Cd}^{2+}$  and  $\text{Cu}^{2+}$  but decreased for  $\text{Pb}^{2+}$  (Fig. S4). Immobilized *Micractinium* sp. (P9-1) displayed decreased removal rates for  $\text{Cd}^{2+}$ , but increased rates for the other two heavy metals (Fig. S3).

Kinetics of the heavy metal removal by free swimming Nordic microalgae were compared to those of the immobilized microalgal-copolymer sorbent (Fig. S6–S11). The removal kinetics of free-swimming microalgae showed a better fit with the pseudo-second-order model than with the pseudo-first-order model, as indicated by higher correlation coefficients; free swimming microalgal strains or the copolymer alone displayed  $R^2$ -values between 0.952 and 1.000, even when only the first hours of the experiment were considered. The adsorption capacities of the free-swimming microalgae were significantly



higher than those of the copolymer alone (without microalgae). According to the modelling results, the copolymer removed per gram 0.154 mg Cd<sup>2+</sup>, 1.296 mg Cu<sup>2+</sup>, and 0.690 mg Pb<sup>2+</sup> from the mixture after 6 h of exposure. In comparison, free swimming *Chlorella vulgaris* (13-1) was able to remove 5.580 mg of cadmium, 69.444 mg of copper and 54.054 mg of lead per gram microalgal biomass (see Table 1). The other microalgal strains were equally efficient. *Coelastrella* sp. (3-4) and *Chlorella sorokiniana* (2-21-1) showed highest adsorption capacities for lead, while the other strains displayed highest removal capacities for copper (Table 1).

Exposure of immobilized microalgae-copolymer sorbent to the heavy metal solution induced shifts in the kinetics; the experimental data were described best by the pseudo-first-order model (Table 1). Only in the case of *Scenedesmus obliquus* (13-8) immobilized to copolymer both kinetic models displayed similar correlation coefficients. Importantly, the experimental data also showed a significant increase in the

adsorption capacities of all microalgae after immobilization. The adsorption capacity of immobilized *Chlorella vulgaris* (13-1) increased 25-fold for cadmium, 4-fold for copper and 1.2-fold for lead. Four immobilized microalgal strains showed increased adsorption capacities only for one or two heavy metal ions in the solution, while  $q_e$  decreased for the third one. Of those *Scenedesmus obliquus* (13-8), *Scotelliopsis reticulata* (UFA-2) and *Micractinium* sp. (P9-1) immobilized to the copolymer displayed reduced adsorption capacities for cadmium, while the calculated values for copper and lead adsorption increased by a factor of 1.2–3 (Table 1). Immobilized *Coelastrella* sp. (3-4) had a slightly reduced adsorption capacity (0.93-fold) for lead, while showing a 6.7-fold increase of  $q_e$  for copper.

### 3.5. Isotherm modelling of heavy metal removal in a multi-elemental mixture

To elucidate the improved heavy metal removal observed with copolymer-immobilized microalgae, the equilibrium inter-

**Table 1** Heavy metal (HM) adsorption capacities ( $q_e$ ) of free-swimming Nordic microalgal strains and copolymer (CP, black) versus microalgal-copolymer sorbent (blue) using pseudo-first and pseudo-second-order kinetic modelling

	HM	Pseudo-first-order			Pseudo-second-order		
		$q_e$ (mg g <sup>-1</sup> )	$k_1$ (h <sup>-1</sup> )	$R^2$	$q_e$ (mg g <sup>-1</sup> )	$k_2$ (g mg <sup>-1</sup> h <sup>-1</sup> )	$R^2$
S/CKO copolymer	Cd <sup>2+</sup>	0.137	0.16	0.966	0.154	2.663	0.996
	Cu <sup>2+</sup>	1.173	0.14	0.963	1.296	0.256	0.997
	Pb <sup>2+</sup>	0.565	0.162	0.922	0.69	0.423	0.983
<i>Scotelliopsis reticulata</i> (UFA-2)	Cd <sup>2+</sup>	10.667	0.417	0.923	15.723	0.138	0.997
	Cu <sup>2+</sup>	25.896	0.203	0.633	39.526	0.05	0.993
	Pb <sup>2+</sup>	19.451	0.212	0.862	24.631	0.039	0.975
<i>Scotelliopsis reticulata</i> (UFA-2) + CP	Cd <sup>2+</sup>	10.625	0.243	0.957	11.682	0.056	0.966
	Cu <sup>2+</sup>	83.873	0.124	0.995	93.46	0.024	0.805
	Pb <sup>2+</sup>	28.855	0.386	0.819	37.879	0.15	0.99
<i>Scenedesmus obliquus</i> (13-8)	Cd <sup>2+</sup>	3.671	0.356	0.897	3.953	0.143	0.956
	Cu <sup>2+</sup>	25.401	0.41	0.837	27.027	0.027	0.952
	Pb <sup>2+</sup>	10.192	0.415	0.988	11.628	0.09	0.996
<i>Scenedesmus obliquus</i> (13-8) + CP	Cd <sup>2+</sup>	3.749	0.201	0.94	6.579	0.341	0.997
	Cu <sup>2+</sup>	90.342	0.211	0.998	105.263	0.007	0.977
	Pb <sup>2+</sup>	15.013	0.462	0.956	18.519	0.1	0.997
<i>Micractinium</i> sp. (P9-1)	Cd <sup>2+</sup>	3.999	1.253	0.876	7.593	0.32	0.999
	Cu <sup>2+</sup>	29.916	0.689	0.838	47.847	0.049	0.998
	Pb <sup>2+</sup>	7.274	0.63	0.934	10.121	0.124	1
<i>Micractinium</i> sp. (P9-1) + CP	Cd <sup>2+</sup>	4.711	0.414	0.977	6.456	0.325	0.997
	Cu <sup>2+</sup>	103.441	0.169	0.996	119.048	0.003	0.947
	Pb <sup>2+</sup>	12.196	0.321	0.957	15.291	0.087	0.994
<i>Coelastrella</i> sp. (3-4)	Cd <sup>2+</sup>	9.614	0.452	0.933	12.077	0.163	0.996
	Cu <sup>2+</sup>	25.803	0.459	0.903	35.211	0.053	0.996
	Pb <sup>2+</sup>	34.536	0.543	0.992	40.984	0.039	0.997
<i>Coelastrella</i> sp. (3-4) + CP	Cd <sup>2+</sup>	20.375	0.253	0.954	28.818	0.052	0.994
	Cu <sup>2+</sup>	236.678	0.307	0.972	243.902	0.002	0.945
	Pb <sup>2+</sup>	38.413	0.431	0.973	49.948	0.012	0.994
<i>Chlorella vulgaris</i> (13-1)	Cd <sup>2+</sup>	3.73	0.589	0.912	5.58	0.411	0.999
	Cu <sup>2+</sup>	56.628	0.846	0.911	69.444	0.023	0.999
	Pb <sup>2+</sup>	45.499	0.228	0.947	54.054	0.013	0.962
<i>Chlorella vulgaris</i> (13-1) + CP	Cd <sup>2+</sup>	140.05	0.069	0.967	142.857	0.001	0.383
	Cu <sup>2+</sup>	272.789	0.115	0.985	434.783	0	0.463
	Pb <sup>2+</sup>	66.427	0.616	0.814	87.719	0.012	0.998
<i>Chlorella sorokiniana</i> (2-21-1)	Cd <sup>2+</sup>	10.694	0.017	0.892	12.24	0.049	0.967
	Cu <sup>2+</sup>	16.296	0.644	0.94	24.51	0.057	0.996
	Pb <sup>2+</sup>	50.174	0.412	0.952	46.083	0.046	0.999
<i>Chlorella sorokiniana</i> (2-21-1) + CP	Cd <sup>2+</sup>	136.811	0.039	0.984	181.818	0	0.044
	Cu <sup>2+</sup>	283.298	0.188	0.995	526.316	0	0.411
	Pb <sup>2+</sup>	69.874	0.261	0.998	78.74	0.007	0.983



**Table 2** Removal of Cd<sup>2+</sup>, Cu<sup>2+</sup> and Pb<sup>2+</sup> in a heavy metal (HM) mixture under equilibrium conditions modelled using the Langmuir or Sips isotherms. Free-swimming Nordic microalgae or the copolymer (CP) alone (black) are compared to copolymer-immobilized microalgae (in blue)

Strain	HM	Langmuir			Sips			
		$q_{\max}$ (mg g <sup>-1</sup> )	$K_L$ (L mg <sup>-1</sup> )	$R^2$	$q_{\max}$ (mg g <sup>-1</sup> )	$K_S$ (L mg <sup>-1</sup> )	nS	$R^2$
S/CKO copolymer	Cd <sup>2+</sup>	1.25	0.074	0.979	10.59	0.013	0.58	0.991
	Cu <sup>2+</sup>	8.67	0.011	0.932	0.92	$5.95 \times 10^{-4}$	4.72	0.972
	Pb <sup>2+</sup>	4.80	0.002	0.977	2.13	$1.59 \times 10^{-2}$	1.72	0.983
<i>Scotelliopsis reticulata</i> (UFA-2)	Cd <sup>2+</sup>	34.33	0.315	0.974	31.07	0.306	1.29	0.979
	Cu <sup>2+</sup>	115.10	0.075	0.953	98.92	0.083	1.08	0.953
	Pb <sup>2+</sup>	1048.00	0.255	0.947	407.00	0.016	3.06	0.980
<i>Scotelliopsis reticulata</i> (UFA-2) + CP	Cd <sup>2+</sup>	361.60	0.080	0.940	237.90	$7.59 \times 10^{-3}$	2.75	0.985
	Cu <sup>2+</sup>	1889.00	0.020	0.961	382.80	0.284	2.24	0.989
	Pb <sup>2+</sup>	1602.00	0.087	0.952	1022.00	0.020	2.42	0.972
<i>Scenedesmus obliquus</i> (13-8)	Cd <sup>2+</sup>	44.69	0.641	0.889	84.83	0.849	0.43	0.971
	Cu <sup>2+</sup>	464.80	0.038	0.958	162.30	0.040	2.02	0.983
	Pb <sup>2+</sup>	1786.00	0.010	0.974	383.80	0.005	2.28	0.988
<i>Scenedesmus obliquus</i> (13-8) + CP	Cd <sup>2+</sup>	107.90	0.088	0.981	138.00	0.083	0.82	0.983
	Cu <sup>2+</sup>	208.80	0.495	0.869	160.90	0.597	3.28	0.993
	Pb <sup>2+</sup>	922.10	0.031	0.916	380.60	$2.32 \times 10^{-4}$	4.15	0.981
<i>Coelastrella</i> sp. (3-4)	Cd <sup>2+</sup>	44.72	0.234	0.969	60.34	0.202	0.98	0.980
	Cu <sup>2+</sup>	814.20	0.019	0.924	148.10	0.029	3.73	0.959
	Pb <sup>2+</sup>	374.10	0.053	0.999	432.20	0.050	0.92	0.999
<i>Coelastrella</i> sp. (3-4) + CP	Cd <sup>2+</sup>	118.10	0.230	0.940	422.70	0.769	0.45	0.990
	Cu <sup>2+</sup>	403.20	0.253	0.910	272.10	0.292	2.37	0.960
	Pb <sup>2+</sup>	881.50	0.037	0.959	403.00	$6.33 \times 10^{-3}$	2.58	0.991
<i>Chlorella vulgaris</i> (13-1)	Cd <sup>2+</sup>	55.20	0.422	0.987	64.95	0.367	0.75	0.996
	Cu <sup>2+</sup>	288.60	0.160	0.982	254.30	0.173	1.12	0.982
	Pb <sup>2+</sup>	140.50	0.140	0.973	164.60	0.137	0.84	0.976
<i>Chlorella vulgaris</i> (13-1) + CP	Cd <sup>2+</sup>	98.59	0.514	0.966	127.50	0.397	0.63	0.989
	Cu <sup>2+</sup>	710.20	0.249	0.932	514.30	0.248	1.89	0.973
	Pb <sup>2+</sup>	850.50	0.041	0.887	391.00	$9.94 \times 10^{-6}$	4.80	0.976
<i>Chlorella sorokiniana</i> (2-21-1)	Cd <sup>2+</sup>	78.48	0.298	0.997	77.36	0.298	1.03	0.997
	Cu <sup>2+</sup>	79.82	0.172	0.999	76.07	0.178	1.05	0.999
	Pb <sup>2+</sup>	665.30	0.036	0.928	307.80	$9.64 \times 10^{-4}$	3.48	0.991
<i>Chlorella sorokiniana</i> (2-21-1) + CP	Cd <sup>2+</sup>	154.40	0.103	0.984	119.70	0.062	1.58	0.996
	Cu <sup>2+</sup>	338.10	0.237	0.969	270.30	0.259	1.41	0.980
	Pb <sup>2+</sup>	1533.00	0.018	0.938	465.90	$6.49 \times 10^{-3}$	3.46	0.996

actions between the adsorbent and adsorbate were examined. Alongside the widely used Langmuir and Freundlich isotherms,<sup>34,35</sup> the Sips and Dubinin–Radushkevich models were also employed, given their potential to more accurately represent the heterogeneous nature of the microalgal surface as an adsorbent. Model suitability was assessed by comparing the correlation coefficients ( $R^2$ ) obtained for each isotherm. Isotherm parameters obtained from the Langmuir and Sips models are shown in Table 2; corresponding data for the Freundlich and Dubinin–Radushkevich models are available in Table S2. Among the models applied, the Sips model provided the best fit across all conditions and consistently outperformed the others based on  $R^2$  values. The Langmuir model yielded relatively high  $R^2$  values, the Freundlich model was not applicable to many of the datasets. The Dubinin–Radushkevich model demonstrated a reasonably good fit. Due to its low removal efficiency and the minimal improvement observed after immobilization, *Micractinium* sp. (P9-1) was excluded from further investigations.

The equilibrium capacities ( $q_{\max}$ ) align with the kinetic values ( $q_e$ , Table 1), confirming the marked enhancement in adsorption capacity after immobilization of the Nordic microalgal strains.

The heavy metal adsorption capacities of *Scotelliopsis reticulata* (UFA-2) and the two *Chlorella* strains – *Chlorella vulgaris* (13-1) and *Chlorella sorokiniana* (2-21-1) – showed the greatest improvement following immobilization. Compared to non-immobilized cells, immobilization enhanced the maximum adsorption capacities by factors ranging from 2.5 to 7.5 for *Scotelliopsis reticulata* (UFA-2), and from 1.5 to 3.5 for the *Chlorella* strains. The adsorption capacities of *Coelastrella* sp. (3-4) and *Scenedesmus obliquus* (13-8) improved for only one or two of the heavy metals in mixture.

### 3.6. The microalgal-copolymer sorbent allows desorption/recovery of heavy metals before reuse

For industrial applications, recovery of the heavy metals as well as reusability of the microalgal-copolymer sorbent is important. After removal of the heavy metals from the aqueous solution, desorption/recovery of the metal ions from the microalgal-copolymer therefore was investigated. Desorption using 0.1 M HNO<sub>3</sub> or 0.1 M EDTA both resulted in high recovery rates of the adsorbed heavy metals (63–98%) from the microalgal-copolymer sorbent (Fig. 6, right panels). While desorption of heavy metals from the copolymer alone was more effective using HNO<sub>3</sub> (Fig. 6A), the use of EDTA resulted in similar or



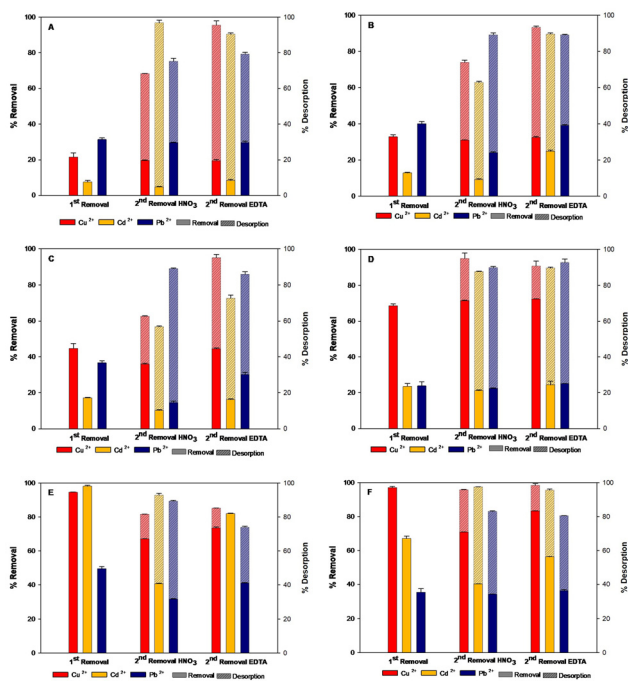


**Fig. 6** Percentage of heavy metal removal (left axis) by S/CKO copolymer alone (A), or copolymer-immobilized microalgae: *Scotiellopsis reticulata* UFA-2 (B), *Scenedesmus obliquus* 13-8 (C), *Coelastrella* sp. 3-4 (D), *Chlorella vulgaris* 13-1 (E) and *Chlorella sorokiniana* 2-21-1 (F). Desorption/recovery of heavy metals (% given on right axis) between the initial round and a second round was performed with either 0.1 M HNO<sub>3</sub> or 0.1 M EDTA.

improved desorption efficiencies of copolymer-immobilized microalgae (Fig. 6B–E). Better heavy metal recovery rates were observed for immobilized spherical microalgae, *i.e.* *Coelastrella* sp. (3-4), *Chlorella vulgaris* (13-1) or *Chlorella sorokiniana* (2-21-1) (Fig. 6D–F), or for the copolymer alone (Fig. 6A), compared to copolymer-immobilized microalgae of the *Scenedesmus* family (Fig. 6B and C).

Regeneration of the microalgae-copolymer will allow multiple reuses of the sorbent. After recovery of the heavy metals and regeneration with CaCl<sub>2</sub>, the microalgal-copolymer sorbents were used in a second round of heavy metal removal. The removal efficiencies of the reused microalgae-copolymer sorbents were comparable to those observed during initial use (Fig. 6). Recovery with 0.1 M EDTA maintained removal performance, while HNO<sub>3</sub> treatment reduced the adsorption capacity of the immobilized microalgal strains *Scotiellopsis reticulata* (UFA-2) and *Scenedesmus obliquus* (13-8); (Table S3). On the other hand, heavy metal removal after HNO<sub>3</sub> treatment decreased more than EDTA treated system in the second round for sorbents using immobilized *Chlorella* strains (Fig. 6E, F and Table S3). For example, after HNO<sub>3</sub> treatment, the removal rates of Cu<sup>2+</sup>, Cd<sup>2+</sup> and Pb<sup>2+</sup> were from 41 to 71% in 13-1 and from 60 to 97% from 2-21-1, while the removal rates in second round after EDTA treatment were comparable to the first application (from 78 to 84% in 13-1 and from 84 to 103% from 2-

21-1). Interestingly, the removal rates of immobilized *Coelastrella* sp. (3-4) even increased (104–106%) in the second round of heavy metal removal (Fig. 6D) after recovery using EDTA. Thus, 0.1 M EDTA allowed both high recovery of the heavy metals from the sorbent (Fig. 6) and high removal rates in a second removal process (Table S3).

## 4. Discussion

Because of their bio-accumulation, biomagnification and half-life of several thousand years, heavy metals cause serious environmental problems.<sup>36</sup> Microbial bioremediation is emerging as a promising strategy for the removal of heavy metal contamination from aqueous environments. In addition to bioremediation, photosynthetic microalgae contribute to oxygen production and the assimilation of nitrogen, phosphate, and carbon dioxide into valuable biomass. The Nordic microalgal strains investigated in this study outperformed commonly studied species – including *Scenedesmus obliquus*, *Chlorella pyrenoidosa*, and *Anabaena flos-aquae* – in their heavy metal adsorption efficiencies.<sup>37</sup> Although many strains effectively adsorb heavy metals under single-element exposure, the presence of multiple metals typically reduces their removal efficiencies, likely due to competition for binding sites on the cell surface.<sup>11,25</sup> Even isolated microalgal cell walls seem to be saturated quickly in the presence of one or two cations, showing low removal values.<sup>19</sup> In binary heavy metal mixtures, *Polyedriopsis spinulosa*, *Tetrademus obliquus*, and *Chlorosarcinopsis bastropiensis* have been reported to remove Pb<sup>2+</sup> more effectively than Cd<sup>2+</sup> or Cu<sup>2+</sup>.<sup>30,38</sup> This preferential uptake of Pb<sup>2+</sup> can be attributed to several factors, including its larger ionic radius, higher polarizability, and classification as a ‘soft acid’ under Hard–Soft Acid–Base (HSAB) theory, which enhances its binding affinity to soft donor groups such as sulfhydryl, carboxyl, and phosphate groups commonly found on microalgal cell surfaces. Moreover, Pb<sup>2+</sup> often forms stronger inner-sphere complexes with cell wall functional groups, leading to more stable binding compared to Cd<sup>2+</sup> and Cu<sup>2+</sup>.<sup>19</sup> Remarkably, in this study, Nordic microalgae could remove Pb<sup>2+</sup>, Cd<sup>2+</sup> and Cu<sup>2+</sup> in complex mixtures relevant for Nordic environments. The affinity of the microalgal strains for individual heavy metals in three-metal mixtures varied depending on the strain, highlighting species-specific differences in metal binding behaviour. While *Chlorella vulgaris* (13-1) and *Chlorella sorokiniana* (2-21-1) showed higher affinity to Cu<sup>2+</sup> and Cd<sup>2+</sup>, *Scotiellopsis reticulata* (UFA-2) had higher affinity to Pb<sup>2+</sup> than to the other heavy metals (Fig. 5 and Fig. S3, S4).

Immobilization of microorganisms to an adequate scaffold has been shown to enhance their removal capacity and to improve their handling. Commonly, the higher biomass density and surface area in immobilized systems can lead to higher treatment rates compared to free-swimming microalgae. Selecting an appropriate scaffold for microalgal immobilization presents several challenges, including issues related



to durability, potential toxicity, and scalability.<sup>11</sup> Traditionally, microalgae have been immobilized on scaffolds like alginate, chitosan or other polymeric compounds.<sup>39,40</sup> Inverse vulcanization copolymers provide a sustainable and adaptable approach for microalgal immobilization, as they are derived from recycled materials. The S/CKO copolymer consisting of S<sub>8</sub> and cooking oil was found to be similar to copolymers synthesized with different vegetable oils,<sup>22,25,32,41</sup> and analogous to that of virgin olive oil<sup>42,43</sup> (Fig. 1), yet, with successful comonomer conversion.<sup>32</sup> Previous studies have demonstrated the ability of inverse vulcanization copolymers to remove heavy metals from aqueous solutions,<sup>44,45</sup> indicating that they can serve not only as a structural scaffold but also as an active component in heavy metal removal. Compared with other adsorbents used for heavy metals removal, including chitosan, S/CKO copolymer alone exhibited lower maximum removal capacities (Table 3). The reader should note, however, that the conditions for the S/CKO copolymer to enhance the removal efficiency were not optimized, contrary to all other adsorbents. Moreover, S/CKO offers notable advantages, such as its sustainable, low-cost nature and its reusability. The S/CKO copolymer exhibited heavy metal adsorption capabilities, with removal efficiencies of up to 70% for Pb<sup>2+</sup>, 35–70% for Cd<sup>2+</sup>, and around 15% for Cu<sup>2+</sup> (Fig. 3). The observed differences can be attributed to the HSAB theory and ionic size, with the copolymer exhibiting greater affinity for the larger, softer cations Pb<sup>2+</sup> and Cd<sup>2+</sup> than for the smaller, harder Cu<sup>2+</sup>.<sup>22,46</sup>

Compared to free-swimming cells, immobilization of Nordic microalgae onto the novel and sustainable S/CKO copolymer not only significantly enhanced their heavy metal removal from complex mixtures but also increased their removal capacity. Furthermore, the microalgae-copolymer sorbent exhibited a higher maximal adsorption capacity than other adsorbents described in literature, such as chitosan, biochars or copolymers (Table 3).<sup>47–50</sup> The S/CKO copolymer proved to be a versatile immobilization scaffold, suitable for

different microalgal species with a wide range of cell walls and their various functional groups (Fig. 4). It demonstrated highest affinity for spherical microalgal strains, such as *Coelastrella* sp. and *Chlorella* strains (Fig. 4C, F and G). Modifying the copolymer with different heteroatoms might improve its affinity for non-spherical microalgae, such as *Scotiellopsis reticulata* or *Scenedesmus obliquus*.<sup>51</sup> Nevertheless, heavy metal removal was enhanced for all 6 strains tested (Fig. 5 and Fig. S1–S5), demonstrating that this copolymer not only can immobilize the different microalgal strains, but also increases their capacity to remove these pollutants from aqueous solutions. Commonly immobilisation of microalgae enhances cell density and thereby improves high-efficient wastewater treatment,<sup>14,52</sup> however, the microalgal-copolymer sorbents indeed displayed enhanced adsorption capacities to remove heavy metals compared to free-swimming microalgae or copolymer alone at similar concentrations.

Since both the copolymer and microalgae are biodegradable and compostable, this sorbent supports a fully sustainable cradle-to-grave cycle, which allows the concentration and recovery of heavy metals from large water bodies. Effective bioremediation requires both high heavy metal recovery and the capacity for repeated use of the sorbent across multiple removal cycles. Structural stability of the sorbent is another critical factor to consider. Regeneration of the system using acids or chelating compounds could degrade the copolymer upon repeated uses. However, inverse vulcanization copolymers have been demonstrated to exhibit high stability and reusability in heavy metal removal cycles involving Au(III) or Hg<sup>2+</sup>, even when acids (HCl) or chelating compounds (thiourea) were employed for desorption processes,<sup>53,54</sup> supporting that the S/CKO copolymer remains structurally intact after regeneration. Similarly, microalgal biomass has successfully been reused in concomitant heavy metal removal cycles employing H<sub>2</sub>SO<sub>4</sub>, HCl, HNO<sub>3</sub> or EDTA during desorption; free-swimming microalgae maintained comparable removal

**Table 3** Comparison of S/CKO copolymer with other adsorbents in mixtures of heavy metals

Adsorbent	Heavy metals	Dosage	Contact time	Q <sub>max</sub> (mg g <sup>-1</sup> )	Reusability	Ref.
Chitosan-Fe <sub>3</sub> O <sub>4</sub> -SiO <sub>2</sub>	Ni <sup>2+</sup>	2.5 g L <sup>-1</sup>	90 min	800.04	No	47
	Co <sup>2+</sup>			1548.73		
	Cu <sup>2+</sup>			78.4		
Chitosan-Kryptofix222	Cd <sup>2+</sup>	100 mg	50 min	340.3	No	48
	Pb <sup>2+</sup>			510		
	Cd <sup>2+</sup>			59.10		
Magnetic microalgal-derived biochar	Cd <sup>2+</sup>	0.6 g L <sup>-1</sup>	24 h	59.10	Yes	49
	Cu <sup>2+</sup>			43.82		
	Zn <sup>2+</sup>			36.35		
	Pb <sup>2+</sup>			147.17		
	Mn <sup>2+</sup>			17.65		
	Cd <sup>2+</sup>			110.92		
Poly[N-(4-[4-(aminophenyl) methylphenylmethacrylamide])]	Ni <sup>2+</sup>	3.0 g L <sup>-1</sup>	30 min	110.92	No	50
	Co <sup>2+</sup>			108.96		
	Cu <sup>2+</sup>			66.09		
S/CKO copolymer	Cd <sup>2+</sup>	20 g L <sup>-1</sup>	6 h	1.25	Yes	This study
	Cu <sup>2+</sup>			8.67		
	Pb <sup>2+</sup>			4.80		
	Cd <sup>2+</sup>			98.59		
S/CKO copolymer + <i>Chlorella vulgaris</i>	Cd <sup>2+</sup>	20 g L <sup>-1</sup>	6 h	98.59	Yes	This study
	Cu <sup>2+</sup>			710.20		
	Pb <sup>2+</sup>			850.50		



capacities across cycles.<sup>55</sup> Structural robustness of both S/CKO copolymer and microalgal biomass under acidic or chelating regeneration conditions therefore can be anticipated, however, further studies are required to confirm the structural stability of the Nordic microalgae/SCKO copolymer system. While 0.1 M HNO<sub>3</sub> treatment resulted in efficient desorption of Cd<sup>2+</sup>, Cu<sup>2+</sup>, and Pb<sup>2+</sup>, it adversely impacted the reusability of the sorbent. Compared to the initial removal rates only about 40–80% of the individual heavy metals were adsorbed in a second cycle. HNO<sub>3</sub>, a strong, corrosive acid, likely affects the microalgae as well as their binding onto the copolymer. Notably, heavy metal binding to dead microalgal biomass was unaffected by HNO<sub>3</sub> stripping over five sorption–desorption cycles<sup>29</sup> suggesting that the negative impact of HNO<sub>3</sub> is more likely related to the immobilization of the microalgae on the surface of the sustainable copolymer matrix. When embedded in alginate, stable heavy metal removal rates were observed over 5–8 sorption–desorption cycles, using HCl for metal stripping.<sup>52,56</sup> However, the reusability of these systems might be limited by the presence of other microorganisms, particularly algicidal bacteria.<sup>57,58</sup> In contrast, copolymers synthesized by inverse vulcanization from elemental sulfur (S<sub>8</sub>) and castor oil have demonstrated antibacterial activity against Gram-negative bacteria, thereby reducing the risk of microbial contamination in large-scale applications.<sup>59</sup>

Treatment with 0.1 M EDTA enabled efficient heavy metal recovery from the microalga-copolymer sorbent and, importantly, maintained the functionality of the sorbent for subsequent reuse cycles. Heavy metal removal of the *Coelastrella* sp. (3-4)-copolymer sorbent even improved after EDTA stripping (Fig. 6 and Table S3). Sorbents containing the two most promising Nordic microalgal species for heavy metal bioremediation, *Chlorella vulgaris* 13-1 and *Chlorella sorokiniana* (2-21-1), maintained high removal efficiencies after EDTA regeneration, even when exposed to the highest metal concentrations tested (5 mg L<sup>-1</sup> Cu<sup>2+</sup>, 2.5 mg L<sup>-1</sup> Cd<sup>2+</sup>, and 3.6 mg L<sup>-1</sup> Pb<sup>2+</sup>; Mix H, Table S1). Specifically, *C. vulgaris* (13-1) removed 78% of Cu<sup>2+</sup>, 84% of Cd<sup>2+</sup>, and 83% of Pb<sup>2+</sup>, while *C. sorokiniana* 2-21-1 achieved 86% Cu<sup>2+</sup>, 84% Cd<sup>2+</sup>, and 103% Pb<sup>2+</sup> removal compared to the first cycle (Table S3). The mechanism underlying this enhanced adsorption remains unclear and will be addressed in future studies. The spherical shape of *Chlorella* cells might contribute to surface enlargements when immobilized (Fig. 6). Additionally, biofilm formation following immobilization could enhance system stability against external stressors such as acids or chelating agents used during desorption. The spherical shape of *Chlorella* cells, together with the production of specific exopolysaccharides (EPS), may be the responsible for the enhanced removal of heavy metals under immobilized conditions (Fig. 6).<sup>60</sup> Biofilm formation is known to be mediated by exopolysaccharides (EPS) and different signalling molecules, such as c-di-GMP.<sup>61,62</sup> However, *Chlorella vulgaris* 13-1 has been reported not to produce EPS.<sup>63</sup> Nevertheless, both *Chlorella* strains exhibited higher immobilization efficiencies than the other species tested, which may account for their superior heavy metal removal performance.<sup>60</sup>

Thus, native Nordic microalgae – particularly *Chlorella* strains – immobilized on a sustainable copolymer, efficiently adsorbed heavy metals at concentrations relevant to Nordic environments,<sup>4</sup> enabling effective removal, recovery, and sorbent reusability.

The removal of heavy metals by microalgae is carried out in two different phases.<sup>64,65</sup> In the first, rapid phase the heavy metals are adsorbed to the microalgal surface; during the slower, second phase, the microalgal surface becomes saturated with metal ions, which are subsequently transported into the cell.<sup>66</sup> Uptake of copper ions into microalgae is performed by highly specific Cu-transporters and cupric reductases.<sup>67</sup> Other metals might be absorbed by non-specific bivalent metal ion transporters as identified in the marine diatom *Thalassiosira pseudonana* or other marine microalgae.<sup>67,68</sup> Here, for the first time, a detailed comparison of a multi-elemental removal by Nordic microalgae is presented comparing the same species either swimming freely in aqueous solution or immobilized to a copolymer. Removal kinetics of free-swimming microalgae exposed to heavy metals were best described by pseudo-second-order kinetics. The pseudo-second-order model was developed to describe adsorption processes involving both surface interactions (physisorption) and potential exchange or transport mechanisms through a permeable surface (chemisorption).<sup>69,70</sup> Pseudo-second-order kinetics earlier had provided an accurate fit for free-swimming microalgae, such as *Chlorella sorokiniana* and *Synechocystis* sp. PCC6803, when cultivated in the presence of a single heavy metal species.<sup>71,72</sup> However, studies like ours, involving multi-elemental systems containing more than two different heavy metals remain scarce.

Equilibrium modelling of heavy metal adsorption describes the relationship between the adsorbent and metal ions near the surface. Identifying the model that best represents the experimental system remains a significant challenge. Each adsorption model is based on specific assumptions about the nature of the adsorbent and its interactions with the adsorbate, leading to differences in their applicability and accuracy. The well-used Langmuir-model assumes that the adsorbent consists of a monolayered homogenous surface containing an even distribution of adsorption sites.<sup>34</sup> In microalgae, different biomolecules *i.e.* proteins, carbohydrates and lipids, are involved in metal binding on the surface, and their concentrations and distributions differ between strain and growth state.<sup>13,20,73</sup> Microalgae therefore exhibit a complex surface structure of multiple layers.<sup>74,75</sup> Nevertheless, this model showed a strong fit for several copolymer-immobilized Nordic microalgae, with *R*<sup>2</sup> values exceeding 0.91 for *Coelastrella* sp., *Scotiellopsis reticulata*, and *Chlorella sorokiniana* (Table 2). Due to its limitation to low or intermediate adsorbate concentrations on heterogeneous surfaces,<sup>76,77</sup> the Freundlich model poorly describes heavy metal adsorption by microalgae or the microalgae-copolymer sorbent, especially for Cu<sup>2+</sup> (Table S2). The Dubinin–Radushkevich isotherm model, based on the assumption of a porous adsorbent surface, provided reasonable fits and appears appropriate for describing heavy metal



interactions with microalgal surfaces. Nonetheless, its assumption of surface heterogeneity can result in lower correlation coefficients (Table S2). The Sips model overcomes several limitations of the previously mentioned isotherm models, particularly in systems involving heterogeneous surfaces. Although it is most applicable at moderate to low adsorbate concentrations, the Sips model effectively accounts for the complexity of surface interactions, enabling a good fit for both microalgal bioremediation and the microalgae-copolymer system. Notably,  $R^2$  values exceeded 0.95 under all tested conditions involving the microalga-copolymer sorbent (Table 2), demonstrating the model's suitability for describing adsorption behaviour in this context. Although the Sips model is not commonly applied to microalgal systems, recent studies suggest that microalgae may form complex monolayer biosorption structures.<sup>13,78</sup> Furthermore, this model has also been shown to effectively describe heavy metal ( $\text{Cu}^{2+}$  and  $\text{Pb}^{2+}$ ) removal in alginate-based algal beads,<sup>79</sup> supporting its broader applicability in algal biosorption systems.

Scalability represents a critical aspect of the system, particularly regarding its potential for industrial application. Previous studies demonstrated that native Nordic microalgae were able to degrade organic pollutants from municipal wastewater in an 880 L open-pond bioreactor, with *Chlorella* identified as the main competing algal species. These findings highlight the robustness of Nordic strains and their adaptation to extreme temperatures and light conditions.<sup>80</sup> In parallel, the low cost and high abundance of waste cooking oil and sulphur extracted from crude oil, which are the monomers of the S/CKO copolymer, facilitate the development of an inexpensive and scalable method for producing the copolymer as scaffold.<sup>81</sup> These conditions underscore the potential of the Nordic microalgae-S/CKO copolymer system as a scalable and promising approach for heavy metals removal. However, further research is required to comprehensively evaluate the economic feasibility and operational processes associated with its high-scale implementation.

## 5. Conclusions

Microalgae immobilized on a copolymer made from recycled waste products achieved highly efficient removal of heavy metals from complex mixtures, highlighting the potential of this approach for environmentally friendly bioremediation. A sustainable copolymer, synthesized by inverse vulcanization using waste cooking oil and sulphur arising from petrochemical wastes from domestic and industrial wastes, was used as a scaffold to immobilize Nordic microalgae, which are adapted to challenging conditions and were shown to outcompete other microalgal strains in their bioremediation performance. Besides the commonly known advantages of immobilisation this microalgal-copolymer sorbent even improved the capacities of the Nordic microalgae to remove copper, cadmium and lead from a mixture at industrial relevant concentrations. After efficient recovery of the heavy metals, the

sorbent was successfully reused in a second round of bioremediation with highly efficient results. This novel system contributes to the circular economy and, at the same time, can remove mixtures of the most hazardous pollutants in aquatic environments. Further studies at high-scale process with industrial wastewaters will be performed to demonstrate the industrial relevance of this process.

## Author contributions

A. L.-V.: conceptualization, methodology, investigation, validation, data curation, formal analysis, visualization, writing – original draft, writing – review & editing. M. P.: conceptualization, methodology, investigation, validation, data curation, formal analysis, visualization, writing – original draft, writing – review & editing. J. C.-C.: methodology, investigation, data curation, formal analysis, writing – review & editing. J. U.: supervision, writing – review & editing. C. F.: conceptualization, funding acquisition, project administration, supervision, writing – original draft, writing – review & editing.

## Conflicts of interest

All authors have read and approved the manuscript and declare no competing interests.

## Data availability

The data supporting this article have been included as part of the supplementary information (SI) or are available upon request.

Supplementary information is available. Removal experiments and kinetics models and data. See DOI: <https://doi.org/10.1039/d5gc03769g>.

## Acknowledgements

The authors are grateful to the Swedish Research Council FORMAS (2019-00492 to CF) and Umeå University as well as the Industrial Doctoral School at Umeå University for their financial support. A. L.-V. also wishes to thank Next Generation European Funds and the Ministry of Universities of Spain for funding the Recualificación del Profesorado Universitario system. J. C.-C. has the benefit of the funding from the Juan de la Cierva grant (JDC2022-050255-I) which is financed by MCIU/AEI/10.13039/501100011033 and the European Union's "NextGenerationEU"/PRTR program.

The authors would further like to thank András Gorzsás from the Vibrational Spectroscopy Core Facility at Umeå University for the provided expertise and the data processing of the FTIR and Raman spectra.



## References

- D. Zhao, Q. Wu, Y. Zeng, J. Zhang, A. Mei, X. Zhang, S. Gao, H. Wang, H. Liu, Y. Zhang, S. Qi and X. Jia, *Int. J. Coal Sci. Technol.*, 2023, **10**, 8.
- H. Wang, C. Wang, B. Ge, X. Zhang, C. Zhou, X. Yan, R. Ruan and P. Cheng, *Chem. Eng. J.*, 2023, **473**, 145274.
- R. Rentz, A. Widerlund, M. Viklander and B. Öhlander, *Water, Air, Soil Pollut.*, 2011, **218**, 651–666.
- S. Fischer, G. Rosqvist and S. R. Chalov, *Sustainability*, 2020, **12**, 1394.
- R. Amils, D. Fernández-Remolar, V. Parro, J. A. Rodríguez-Manfredi, M. Oggerin, M. Sánchez-Román, F. J. López, J. P. Fernández-Rodríguez, F. Puente-Sánchez, C. Briones, O. Prieto-Ballesteros, F. Tornos, F. Gómez, M. García-Villadangos, N. Rodríguez, E. Omoregie, K. Timmis, A. Arce, J. L. Sanz and D. Gómez-Ortiz, *Life*, 2014, **4**, 511–534.
- E. S. Salama, H. S. Roh, S. Dev, M. A. Khan, R. A. I. Abou-Shanab, S. W. Chang and B. H. Jeon, *World J. Microbiol. Biotechnol.*, 2019, **35**, 1–19.
- H. T. T. Nguyen, D. A. Jadhav, T. Eisa, H. Y. Nguyen, G. T. H. Le, T. T. Q. Le, M. R. Jae, K. S. Khoo, E. Yang and K. J. Chae, *Process Saf. Environ. Prot.*, 2024, **190**, 212–225.
- S. S. Mahmood, M. M. Al-Rajabi, P. M. Abdul, G. Ding, K. F. Kamarudin, A. A. N. Gunny, J. P. Tan and M. S. Takriff, *Algal Res.*, 2025, **85**, 103839.
- J. Zhao, L. Peng and X. Ma, *Environ. Res.*, 2025, **266**, 120560.
- M. M. El-Sheekh, H. Y. El-Kassas and S. S. Ali, *Microb. Cell Fact.*, 2025, **24**, 19.
- M. Han, C. Zhang and S. H. Ho, *Environ. Sci. Ecotechnology*, 2023, **14**, 100227.
- A. León-Vaz, R. León, J. Vigara and C. Funk, *New Biotechnol.*, 2023, **73**, 1–8.
- M. Plöhn, C. Escudero-Oñate and C. Funk, *Algal Res.*, 2021, **59**, 102471.
- Z. Chen, A. I. Osman, D. W. Rooney, W. Oh and P. Yap, *Sustainability*, 2023, **15**, 5128.
- B. Xie, X. Tang, H. Y. Ng, S. Deng, X. Shi, W. Song, S. Huang, G. Li and H. Liang, *Chem. Eng. J.*, 2020, **388**, 124217.
- C. Y. Chen, E. W. Kuo, D. Nagarajan, C. Di Dong, D. J. Lee, S. Varjani, S. S. Lam and J. S. Chang, *Bioresour. Technol.*, 2021, **326**, 124773.
- R. Wang, F. Li, W. Ruan, Y. Tai, H. Cai and Y. Yang, *Biochem. Eng. J.*, 2020, **161**, 107700.
- J. Wang, Q. Tian, L. Cui, J. Cheng, H. Zhou, Y. Zhang, A. Peng and L. Shen, *J. Hazard. Mater.*, 2023, **445**, 130507.
- O. Spain, M. Plöhn and C. Funk, *Physiol. Plant.*, 2021, **173**, 526–535.
- O. Spain and C. Funk, *J. Agric. Food Chem.*, 2022, **70**, 9711–9721.
- W. J. Chung, J. J. Griebel, E. T. Kim, H. Yoon, A. G. Simmonds, H. J. Ji, P. T. Dirlam, R. S. Glass, J. J. Wie, N. A. Nguyen, B. W. Guralnick, J. Park, Á. Somogyi, P. Theato, M. E. Mackay, Y. E. Sung, K. Char and J. Pyun, *Nat. Chem.*, 2013, **5**, 518–524.
- J. Cubero-Cardoso, A. A. Cuadri, F. G. Feroso, J. E. Martín-Alfonso and J. Urbano, *ACS Appl. Polym. Mater.*, 2022, **4**, 3667–3675.
- A. Hoefling, Y. J. Lee and P. Theato, *Macromol. Chem. Phys.*, 2017, **18**, 1600303.
- M. González-Hourcade, D. Fernando and F. G. Gentili, *Algal Res.*, 2023, **75**, 103254.
- A. Leon-Vaz, J. Cubero-Cardoso, Á. Trujillo-Reyes, F. G. Feroso, R. León, C. Funk, J. Vigara and J. Urbano, *Chemosphere*, 2023, **315**, 137761.
- L. Ferro, F. G. Gentili and C. Funk, *Algal Res.*, 2018, **32**, 44–53.
- E. H. Harris, *Chlamydomonas Sourceb.*, 2009, 241–302.
- D. Malyshev, C. C. Lee and M. Andersson, *Microsc. Microanal.*, 2024, **30**, 564–573.
- H. Li, H. Sun, J. Wang, X. Ma and Q. Wei, *Biochem. Eng. J.*, 2024, **207**, 109336.
- Y. Ding, R. He, C. Wang, Q. Wei, X. Ma and G. Yang, *J. Water Process Eng.*, 2024, **60**, 105207.
- P. K. Revelou, M. Xagoraris, A. Alexandropoulou, C. D. Kanakis, G. K. Papadopoulos, C. S. Pappas and P. A. Tarantilis, *Molecules*, 2021, **26**, 1–13.
- S. F. Valle, A. S. Giroto, R. Klaic, G. G. F. Guimarães and C. Ribeiro, *Polym. Degrad. Stab.*, 2019, **162**, 102–105.
- F. Lia, B. Vella, M. Z. Mangion and C. Farrugia, *Foods*, 2020, **9**, 1–14.
- I. Langmuir, *J. Am. Chem. Soc.*, 1919, **40**, 1361–1403.
- H. Freundlich, *Z. Phys. Chem.*, 1907, **57**, 385–470.
- R. M. Fisher and V. Gupta, Heavy Metals, in *StatPearls [Internet]*, StatPearls Publishing, Treasure Island (FL), 2024.
- M. Wang, H. Gui, J. Chen, C. Li, C. Wang, C. Chen, C. Zhao and Y. Li, *Pol. J. Environ. Stud.*, 2022, **31**, 1847–1855.
- M. Nanda, K. K. Jaiswal, V. Kumar, M. Verma, M. S. Vlaskin, P. Gururani, H. Kim, M. F. Alajmi and A. Hussain, *J. Water Process Eng.*, 2021, **44**, 102404.
- S. Vasilieva, K. Shibzukhova, A. Morozov, A. Solovchenko, I. Bessonov, M. Kopitsyna, A. Lukyanov, K. Chekanov and E. Lobakova, *J. Biotechnol.*, 2018, **281**, 31–38.
- Y. Li, X. Wu, Y. Liu and B. Taidi, *World J. Microbiol. Biotechnol.*, 2024, **40**, 150.
- A. Nayeem, M. F. Ali and J. H. Shariffuddin, *Chem. Eng. Technol.*, 2022, **45**, 971–978.
- A. Rohman and Y. B. C. Man, *Food Res. Int.*, 2010, **43**, 886–892.
- M. S. Sarjadi, T. C. Ling and M. S. Khan, *J. Phys.: Conf. Ser.*, 2019, **1358**, 012007.
- F. G. Müller, L. S. Lisboa and J. M. Chalker, *Adv. Sustainable Syst.*, 2023, **7**, 2300010.
- Y. Ma, C. Shi, Q. Hong, J. Du, H. Zhang, X. Zheng, Z. Qu, X. Zhang and H. Xu, *Sep. Purif. Technol.*, 2025, **362**, 131902.
- A. Haro-Martínez, R. Arroyo-Carrasco, L. Galvan, A. Sayago, A. A. Cuadri, E. Martín-Alfonso, A. Trujillo-Reyes, F. G. Feroso, J. Cubero-Cardoso and J. Urbano, *Chem. Eng. J.*, 2023, **470**, 143905.



- 47 D. A. Ali and R. G. Ali, *BMC Chem.*, 2024, **18**, 147.
- 48 A. A. Saaid and B. M. Ibrahim, *Int. J. Biol. Macromol.*, 2025, **320**, 146124.
- 49 X. Tian, S. Chu, Y. Hu, L. Luo, X. Lin and H. Wang, *J. Water Process Eng.*, 2025, **69**, 106622.
- 50 A. K. Kushwaha, N. Gupta and M. C. Chattopadhyaya, *Arabian J. Chem.*, 2017, **10**, S1645–S1653.
- 51 A. P. Grimm, M. Plank, A. Stihl, C. W. Schmitt, D. Voll, F. H. Schacher, J. Lahann and P. Théato, *Angew. Chem., Int. Ed.*, 2024, **63**, e202411010.
- 52 A. Ahmad, A. H. Bhat and A. Buang, *J. Cleaner Prod.*, 2018, **171**, 1361–1375.
- 53 Z. Ren, X. Jiang, L. Liu, C. Yin, S. Wang and X. Yang, *J. Mol. Liq.*, 2021, **328**, 115437.
- 54 Y. Chen, A. Yasin, Y. Zhang, X. Zan, Y. Liu and L. Zhang, *Materials*, 2020, **13**, 632.
- 55 P. Sarwa and S. K. Verma, *Clean: Soil, Air, Water*, 2014, **42**, 1298–1303.
- 56 M. A. Hashim, H. N. Tan and K. H. Chu, *Sep. Purif. Technol.*, 2000, **19**, 39–42.
- 57 C. Liao, X. Liu, R. Liu and L. Shan, *Appl. Biochem. Biotechnol.*, 2015, **177**, 567–576.
- 58 C. Liao and X. Liu, *Water, Air, Soil Pollut.*, 2014, **225**, 2120.
- 59 J. Cubero-Cardoso, P. Gómez-Villegas, M. Santos-Martín, A. Sayago, Á. Fernández-Recamales, R. Fernández de Villarán, A. A. Cuadri, J. E. Martín-Alfonso, R. Borja, F. G. Feroso, R. León and J. Urbano, *Polym. Test.*, 2022, **109**, 1–8.
- 60 K. Xu, H. Yu, Z. Zhu, Z. Shen and X. Zou, *J. Environ. Chem. Eng.*, 2025, **13**, 119398.
- 61 X. Liu, B. Cao, L. Yang and J. Gu, *Biotechnol. Adv.*, 2022, **56**, 107915.
- 62 X. Liu, L. Zou, B. Li, P. Di Martino, D. Rittschof, J. Yang, J. Maki, W. Liu and J. Gu, *Nat. Chem. Biol.*, 2024, **20**, 1406–1419.
- 63 O. Spain and C. Funk, *Algal Res.*, 2024, **79**, 103450.
- 64 D. Mahlangu, K. Mphahlele, F. De Paola and N. H. Mthombeni, *Water*, 2024, **16**, 1–23.
- 65 Y. Wang, J. Ma, H. Chu, X. Zhou and Y. Zhang, *Chem. Eng. J.*, 2024, **483**, 149222.
- 66 Y. K. Leong and J. S. Chang, *Bioresour. Technol.*, 2020, 122886.
- 67 L. Kong, *Microorganisms*, 2022, **10**, 1853.
- 68 J. Guo, B. R. Green and M. T. Maldonado, *Protist*, 2015, **166**, 58–77.
- 69 W. Shi, Z. Wang, F. Li, Y. Xu and X. Chen, *Chemosphere*, 2023, **329**, 138596.
- 70 K. Sbihi, S. Elhamji, S. Lghoul, K. Aziz, A. El Maallem, J. Mabrouki, M. El-sheekh and F. Aziz, *Sustainability*, 2024, **16**, 918.
- 71 L. Shen, J. Wang, Z. Li, L. Fan, R. Chen, X. Wu, J. Li and W. Zeng, *J. Water Process Eng.*, 2020, **33**, 101026.
- 72 A. Petrovic and M. Simonovic, *Int. J. Environ. Sci. Technol.*, 2016, **13**, 1761–1780.
- 73 A. Shchukarev, Z. Gojkovic, C. Funk and M. Ramstedt, *Appl. Surf. Sci.*, 2020, **526**, 146538.
- 74 P.-H. Baudelet, G. Ricochon, M. Linder and L. Muniglia, *Algal Res.*, 2017, **25**, 333–371.
- 75 T. M. Radic, P. Vukosav, A. Cackovic and A. Dulebo, *Water*, 2023, **15**, 1983.
- 76 X. Sun, H. Huang, Y. Zhu, Y. Du, L. Yao and X. Jiang, *Colloids Surf., A*, 2019, **583**, 123926.
- 77 Y. Liu and Y.-J. Liu, *Sep. Purif. Technol.*, 2008, **61**, 229–242.
- 78 M. D. R. Martínez-Macias, O. Nateras-Ramírez, J. López-Cervantes, D. I. Sánchez-Machado, D. O. Corona-Martínez, R. G. Sánchez-Duarte, M. A. Correa-Murrieta and R. J. Aguilar-Ruiz, *J. Appl. Phycol.*, 2024, **36**, 1339–1352.
- 79 S. Wang, T. Vincent, C. Faur and E. Guibal, *Bioresour. Technol.*, 2017, **231**, 26–35.
- 80 S. Lage, A. Toffolo and F. G. Gentili, *Chemosphere*, 2021, **276**, 130122.
- 81 S. Afonso and H. Mutlu, *Eur. J. Lipid Sci. Technol.*, 2025, **127**, e70018.

